



## Virus-mimetic polymeric micelles for targeted siRNA delivery

Xiao-Bing Xiong<sup>a</sup>, Hasan Uludağ<sup>b</sup>, Afsaneh Lavasanifar<sup>a,b,\*</sup>

<sup>a</sup> Faculty of Pharmacy and Pharmaceutical Sciences, University of Alberta, Edmonton, AB T6G 2N8, Canada

<sup>b</sup> Department of Chemical and Materials Engineering, Faculty of Engineering, University of Alberta, Edmonton, AB, Canada

### ARTICLE INFO

#### Article history:

Received 23 March 2010

Accepted 30 March 2010

Available online 27 April 2010

#### Keywords:

Polymeric micelles  
siRNA delivery  
Drug targeting  
Multidrug resistance  
P-glycoprotein

### ABSTRACT

In this study, an engineered non-viral polymer based delivery systems with structural features mimicking that of viral vectors was developed and the potential of this carrier for siRNA delivery was assessed. The developed siRNA carrier was based on poly(ethylene oxide)-*block*-poly( $\epsilon$ -caprolactone) (PEO-*b*-PCL) micelles decorated with integrin  $\alpha v \beta 3$  targeting peptide (RGD4C) and/or cell penetrating peptide (TAT) on the PEO shell, and modified with a polycation (spermine) in the PCL core for siRNA binding and protection. We observed increased cellular uptake and effective endosomal escape of siRNA delivered with the peptide-functionalized micelles especially those with dual functionality (RGD/TAT-micelles) compared to unmodified micelles (NON-micelles) in MDA435/LCC6 resistant cells. Transfection of *mdr1* siRNA formulated in peptide-modified micelles led to P-gp down regulation both at the mRNA and protein level. Subsequent to P-gp down regulation, increased cellular accumulation of P-gp substrate, doxorubicin (DOX), in the cytoplasm and nucleus of resistant MDA435/LCC6 cells after treatment with peptide decorated polymeric micelle/*mdr1* siRNA complexes was observed. As a result, resistance to DOX was successfully reversed. Interestingly, RGD/TAT-micellar siRNA complexes produced improved cellular uptake, P-gp silencing, DOX cellular accumulation, DOX nuclear localization and DOX induced cytotoxicity in MDA435/LCC6 cells when compared to micelles decorated with individual peptides. Results of this study indicated a potential for RGD/TAT-functionalized virus-like micelles as promising carriers for efficient delivery of *mdr1* siRNA to MDA435/LCC6 resistant cells as means to reverse the P-gp mediated multidrug resistance to DOX.

© 2010 Elsevier Ltd. All rights reserved.

### 1. Introduction

RNA interference (RNAi) induced by small interfering RNA (siRNA) has spurred interest as a potential therapeutic tool for knocking down the genes related to human diseases through a post-transcriptional silencing mechanism [1,2]. This strategy offers a new avenue with great potential especially in the therapy of cancer where specific inhibition of oncogenes is desired [3,4]. However, there are a series of hurdles to be overcome before RNAi and their synthetic equivalent (siRNA) can be used in the clinic as anticancer agents [5–7]. Perhaps the most crucial and complex question is how the functional siRNAs can be efficiently delivered to their targets in the cancer cells especially after systemic administration *in vivo*. In contrast to the direct accessibility of localized targets, the metastatic tissue can only be reached through the systemic administration of delivery agents in the bloodstream.

\* Corresponding author. Faculty of Pharmacy and Pharmaceutical Sciences, University of Alberta, Edmonton, AB T6G 2N8, Canada. Tel.: +1 780 492 2742; fax: +1 780 492 1217.

E-mail address: [alavasanifar@pharmacy.ualberta.ca](mailto:alavasanifar@pharmacy.ualberta.ca) (A. Lavasanifar).

Therefore, the effective use of siRNAs in cancer therapy will be dependent on the development of a delivery vehicle that can be systemically administered. Such delivery system should be safe for systemic use, and be able to avoid rapid elimination from circulation, protect siRNA from enzymatic degradation by endogenous nucleases and finally preferentially accumulate in both primary and metastatic tumor sites by the enhanced permeability and retention (EPR) effect [8–10]. Moreover, because siRNA requires cellular internalization, accumulation within the tumor microenvironment would not be sufficient for a therapeutic outcome. Selective interaction with cancer cells, passage through the cell membrane and timely unpacking of complexed siRNA from its carrier within the cytoplasm of cancer cells are also critical [11–14].

Viral gene vectors, such as retroviruses and adenoviruses, have been adopted for siRNA delivery since they have high transfection efficiency. However, safety concerns and a negative public perception of viral vectors are currently impeding the further development of these vehicles and limit their entry into new clinical trials [15,16]. Seeking alternative siRNA vectors with viral-like high transfection efficiency remains a great challenge. Favorable safety profile and possibility for the engineering of polymer

based nano-carriers, makes them attractive alternatives to viral vectors for the purpose of siRNA delivery [12].

Polymeric micelles self-assembled from amphiphilic block copolymers are promising carriers for cancer targeting due to their nanoscopic dimension, segregated core/shell structure, protective effect of the hydrophobic core on encapsulated drugs and stealth properties induced by their hydrophilic shell [17–19]. We have developed a new family of biodegradable amphiphilic poly(ethylene oxide)-*block*-poly( $\epsilon$ -caprolactone) (PEO-*b*-PCL) copolymers with grafted polyamines on their PCL block (noted as PEO-*b*-P(CL-*g*-polyamine)) that have shown promise in forming polyion complex (PIC) micelles with siRNA. The PEO-*b*-P(CL-*g*-polyamine) micelles were found to be efficient in the protection of siRNA against degradation in serum and the delivery of *mdr1* siRNA to silence P-glycoprotein (P-gp) expression in human MDA435/LCC6 resistant cancer cell line [20]. The PIC micellar vectors, however, required high doses of *mdr1* siRNA (>200 nM) to achieve significant down regulation of P-gp in cancer cells, which may cause off-target gene silencing effects [21]. This observation was attributed to the slow interaction and internalization of polymeric micellar vectors by cancer cells introduced by the steric effect of the hydrophilic PEO shell that acts as a barrier for the attachment of micellar carrier to cells.

In this paper, functionalization of the micellar surface with an integrin  $\alpha v\beta 3$  ligand (RGD4C) and/or cell penetrating ligand (TAT), both of which used by viruses for cell attachment and entry, has been pursued to correct this shortcoming and at the same time introduce selectivity for the complexed siRNA for cancer cells that over express  $\alpha v\beta 3$  integrin. Based on the common structural features between the peptide decorated PIC micelles and viral vectors (such as nanometer size range, a centrally protected RNA core and peptide ligand on surface), the modified PIC/siRNA micelles especially those with dual modifications (both RGD and TAT peptides) on their surface were hypothesized to be more efficient transfecting agents in cancer cells expressing  $\alpha v\beta 3$  integrin. The validity of this hypothesis was evaluated in this study.

## 2. Materials and methods

### 2.1. Materials and cell lines

The scrambled siRNA (Silencer<sup>®</sup> Negative siRNA), FAM-labeled scrambled siRNA (Silencer<sup>®</sup> FAM<sup>™</sup>-labeled Negative siRNA), and the anti-*mdr1* siRNA (*mdr1* siRNA) were purchased from Ambion (Austin, TX). RGD4C (KACDCRGDCFCG) and TAT peptide (CGRKKRRQRRR) were purchased from Anaspec (Torrance, CA). Trifectin<sup>®</sup> was purchased from Integrated DNA Technologies, Inc (IA, USA). 3-(4,5-dimethylthiazol-2-yl)-2,5-diphenyltetrazolium bromide (MTT). The metastatic human MDA435/LCC6 cancer cells transfected with *mdr1* gene and overexpressing P-glycoprotein (P-gp), were a gift from the laboratory of Dr. Clarke (Georgetown University Medical School, Washington, DC) [22,23]. Cell culture media RPMI 1640, penicillin–streptomycin, fetal bovine serum, L-glutamine and HEPES buffer solution (1 M) were purchased from GIBCO, Invitrogen Corp (USA). All other chemicals were reagent grade. Cells were grown as adherent cultures and maintained in RPMI 1640 supplemented with 10% fetal bovine serum at 37 °C and 5% CO<sub>2</sub>.

### 2.2. Synthesis of acetal-PEO-*b*-P(CL-*g*-SP) and acetal-, RGD4C- or TAT-attached PEO-*b*-P(CL-*g*-DP)

Acetal-PEO-*b*-poly( $\alpha$ -carboxyl- $\epsilon$ -caprolactone) (acetal-PEO-*b*-PCCL) was synthesized as previously reported [24]. Acetal-PEO-*b*-PCL with grafted spermine and N,N-dimethyldipropylentriamine (DP) (acetal-PEO-*b*-P(CL-*g*-SP) and acetal-PEO-*b*-P(CL-*g*-DP), respectively) were synthesized from acetal-PEO-*b*-PCCL as previously reported [20]. After purification, the synthesis of acetal-PEO-*b*-P(CL-*g*-SP) and acetal-PEO-*b*-P(CL-*g*-DP) was confirmed by <sup>1</sup>H NMR.

Conjugation of TAT and RGD4C to the PEO terminus of PEO-*b*-P(CL-*g*-DP) was performed according to the procedure established earlier in our lab [24,25]. Briefly, acetal-PEO-*b*-P(CL-*g*-DP) were assembled into micelles by solvent evaporation method. The micellar solution of acetal-PEO-*b*-P(CL-*g*-DP) (5 mg mL<sup>-1</sup>) was acidified to pH 2.0 with diluted HCl (0.5 mol/L) and stirred for 2 h at room temperature to produce aldehyde-PEO-*b*-P(CL-*g*-DP) micelles. The resulted solution was then neutralized with NaOH (0.5 mol L<sup>-1</sup>), buffered by concentrated sodium phosphate

buffer solution to obtain a 4 mg/mL polymer concentration (pH7.0, ionic strength 0.1 M). The peptide (TAT or RGD4C) was then added and incubated with the aldehyde-micelles at peptide:polymer molar ratio of 1:5 at room temperature for 2 h under moderate stirring. Subsequently, NaBH<sub>3</sub>CN (10 eq.) was added to the polymer and reacted for 90 h to reduce the Schiff base. The conjugation efficiency of TAT and RGD4C peptide to the polymers was assessed by a gradient RP-HPLC method. Unreacted peptide and reducing reagent were removed by extensive dialysis against water. The resulted solution was freeze-dried to get RGD4C- or TAT-PEO-*b*-P(CL-*g*-DP) polymers.

### 2.3. Preparation of polyplex micelles and surface functionalization

Our previous study showed that PEO-*b*-PCL with grafted spermine as the siRNA carrier resulted in better transfection efficiency with less toxicity against MDA435/LCC6 cells as compared to DP grafted copolymers [20]. Therefore, acetal-PEO-*b*-P(CL-*g*-SP) was used to complex siRNA by incubating siRNA with acetal-PEO-*b*-P(CL-*g*-SP) (1:8 weight ratio of siRNA to polymer) in HEPES buffer solution (pH 6.5) at 37 °C for 10 min. For the micellar shell functionalization, either RGD4C-PEO-*b*-P(CL-*g*-DP), TAT-PEO-*b*-P(CL-*g*-DP) or both of them were added to the resulted polymer/siRNA complex and incubated at 37 °C for 30 min. The final weight ratio of siRNA to polymer for all the formulations was adjusted to 1:16 using acetal-PEO-*b*-P(CL-*g*-DP). The polymer ratios used for preparing non-functionalized micelles (NON-micelles) or peptide-functionalized micelles (i.e. RGD-micelles, TAT-micelles, and RGD/TAT-micelles) are listed in Table 1. The particle size of the resulted micelles was determined by a dynamic light scattering (DLS) spectrometer (Malvern Zetasizer 3000, UK) at a polymer concentration of 4 mg/mL.

### 2.4. Cellular uptake of FAM-siRNA/polymer complex micelles

To determine the cellular uptake, resistant MDA435/LCC6 cells were seeded into 12-well plates and incubated at 37 °C until 70% confluence reached. FAM-siRNA (200 nM) formulated in NON-, RGD-, TAT- and RGD/TAT-micelles were added to the wells and incubated for 3 h at 37 °C. The medium was aspirated and cells were rinsed twice with cold PBS. The cells were then trypsinized, washed with cold PBS, filtered through 35  $\mu$ m nylon mesh, and finally examined on a FACSort<sup>™</sup> flowcytometer (Becton–Dickinson Instruments, Franklin Lakes, NJ). Flowcytometry and sorting were performed on a FACS using a 488 nm Ar laser and FL1 bandpass emission for the green FAM-siRNA (530  $\pm$  20). For confocal microscopic observation, MDA435/LCC6 resistant cells were grown on coverslips to 50% confluence and incubated with FAM-siRNA formulated in the above-mentioned micelles or in Trifectin<sup>®</sup> (containing 200 nM siRNA) diluted in appropriate culture medium at 37 °C for 3 h, separately. The cells were then washed twice with PBS, fixed in paraformaldehyde in PBS for 10 min, and then treated with DAPI (excitation/emission: 345/661 nm) for 15 min for nuclei staining. To observe the intracellular distribution of the micelles, cells were incubated with LysoTracker<sup>®</sup> red (50 nM, Molecular Probe, Invitrogen Co., OR, USA) for 0.5 h at the end of uptake study for endosome/lysosome labeling. The cells were imaged by a Zeiss 510 LSMNLO confocal microscope (Carl Zeiss Microscope systems, Jena, Germany) with identical settings for each confocal study.

### 2.5. Transfection with *mdr1* siRNA

MDA435/LCC6 resistant cells were seeded on 12-well plates and incubated till 50% confluence were obtained. After the medium was replaced with fresh medium containing 100 nM of siRNA formulated in micelles and incubated with the cells for 48 h. Cells were also transfected by siRNA formulated in Trifectin<sup>®</sup> as the control according to the manufacturer's protocol. Briefly, siRNA (4  $\mu$ L, 5  $\mu$ M) was incubated with OPTI-Mem<sup>®</sup> (46  $\mu$ L, Invitrogen) for 5 min, followed by incubation with Trifectin<sup>®</sup> (8  $\mu$ L) dissolved in OPTI-Mem<sup>®</sup> (42  $\mu$ L) for 10 min at room temperature. The resulted solution was mixed with 900  $\mu$ L fresh media without antibiotics.

### 2.6. Real-time PCR (RT-PCR)

After 48 h of *mdr1* siRNA transfection (100 nM), total RNA was extracted using RNeasy<sup>™</sup> spin columns (Qiagen, Mississauga, ON, Canada) according to the manufacturer's recommendations. Real-time reverse transcription-polymerase chain reaction (RT-PCR) was conducted using Power SYBRs Green PCR Master Mix (ABI, Foster, CA, USA) in a 25  $\mu$ L of tube with a total reaction volume of 25  $\mu$ L containing first strand reaction product (1  $\mu$ L of a 1:2 dilution), gene specific upstream and

**Table 1**  
Composition and particle size of siRNA complexed micelles.

Micelles	Composition (weight ratio) <sup>a</sup>	Particle size <sup>b</sup> (nm)
NON-micelle/siRNA	I:II:siRNA (8:8:1)	84.5
RGD-micelle/siRNA	I:II:III:siRNA (8:4:4:1)	90.3
TAT-micelle/siRNA	I:II:IV:siRNA (8:4:4:1)	87.8
RGD/TAT-micelle/siRNA	I:III:IV:siRNA (8:4:4:1)	89.9

<sup>a</sup> For the chemical structure of polymers (I, II, III and IV) please refer to fig. 1.

<sup>b</sup> Measured using dynamic light scattering technique.

downstream primers (0.4  $\mu\text{M}$ ). Amplification and analysis of complementary DNA (cDNA) fragments were carried out using a 7300 RT-PCR system (ABI). Cycling conditions were initial denaturation at 95 °C for 3 min, followed by 40 cycles consisting of a 15-s denaturation interval at 95 °C and a 30 s interval for annealing and primer extension at 60 °C. Amplification of the housekeeping gene hypoxanthine-guanine-phosphoribosyltransferase (HPRT) mRNA, which served as a normalization standard, was carried out with HPRT primers (5'-GACCAGTCAACAGGGGACA-3') and (5'-ACACTTCGTGGGGTCCTTTT-3'). The gene specific primers for *mdr1* were MDR1-fwd 5'-ATATCAGCAGCCCATCAT and MDR1-rev 5'-GAAGACTGGATGTCGGGT. Levels of mRNA were measured as CT threshold levels and normalized with the individual HPRT control CT values. Altered mRNA levels in cells are indicated as a 'fold change' compared with control cells. Each sample was measured at least three times.

### 2.7. P-glycoprotein expression

MDA435/LCC6 resistant cells seeded in 8-well plate were transfected by *mdr1* siRNA formulated in NON-, RGD-, TAT-, RGD/TAT-micelles or in Trifectin® for 48 h. The cells were washed with PBS, trypsinized and resuspended in 5% BSA in PBS (500  $\mu\text{L}$ ), and incubated with FITC-labeled anti-human P-gp antibody (20  $\mu\text{L}$ ) for 30 min at 4 °C. After that, cells were washed three times with cold PBS buffer, and the P-gp level was measured by a Becton–Dickinson FACSsort™ flowcytometer [20]. The P-gp level was also examined by fluorescence microscopy Axiocvert 200 M (Carl Zeiss, Germany). Toward this, the *mdr1* siRNA transfected cells grown on coverslips were washed with fresh medium and stained with FITC-labeled anti-human P-gp antibody (20  $\mu\text{L mL}^{-1}$ ) for another 30 min at 4 °C. The cells were then rinsed three times with PBS, fixed in paraformaldehyde in PBS for 10 min, and examined by fluorescence microscopy.

### 2.8. DOX cellular accumulation

After *mdr1* siRNA transfection, DOX cellular uptake was quantified according to the reported method with slight modification [23]. Briefly, the cells were incubated with DOX solution (5  $\mu\text{g mL}^{-1}$ ) for 4 h at 37 °C. The medium was aspirated and cells were rinsed with cold PBS three times. The cells were lysed with PBS containing 1% Triton X-100. DOX concentrations in the cell lysates were measured with a fluorescence spectrophotometer (fluorescence concentration analyzer, Baxter, United States) at an excitation wavelength (485 nm) and an emission wavelength (585 nm). To offset the background fluorescence from the cellular components, separate standardization curves were prepared using cellular lysates containing series of known concentrations of DOX and micellar DOX. Cellular uptake is expressed as nmol per milligram of protein. Protein concentrations of the cell lysates were determined by the Micro BCA™ Protein Assay Reagent Kit (Pierce, Rockford, IL).

### 2.9. Cytotoxicity assay

To evaluate the multidrug resistance reversal, growth medium RPMI 1640 (100  $\mu\text{L}$ ) containing 4000 cells was placed in each well in 96-well plates and incubated overnight to allow cell attachment. Cells were then transfected with *mdr1* siRNA or scramble siRNA formulated in NON-micelles, RGD-micelles, TAT-micelles and RGD/TAT-micelles (100 nM siRNA) or in Trifectin® (40 nM siRNA) for 48 h. Cells without any transfection were used as the control. The medium was then replaced with DOX solution (100  $\mu\text{L}$ , 5  $\mu\text{g mL}^{-1}$ ) and incubated for another 48 h, followed by the addition of MTT solution (20  $\mu\text{L}$ ). Three hours later, medium was aspirated and the precipitated formazan was dissolved in DMSO (200  $\mu\text{L}$ ). Cell viability was determined by measuring the optical absorbance differences between 570 and 650 nm using a PowerwaveX340 microplate reader (BIO-TEK Instruments, Inc., Nepean, Ontario, Canada). The mean and standard deviation of cell viability for each treatment was determined, converted to the percentage of viable cells relative to the untreated control.

## 3. Results and discussion

An efficient and safe siRNA carrier suitable for systemic administration will accelerate the clinical use of siRNA. Multifunctional polymeric micelles with tailored core and shell have been extensively used for cancer targeted delivery of drugs and genetic cargoes [26–29]. Development of PEO-*b*-poly(L-aspartate acid) (PEO-*b*-PAsp) micelles containing diamine side chain in the PAsp block for siRNA complexation and cytoplasmic delivery has been reported by Kataoka et al. [26]. Same research group has also reported on the conjugation of the cyclic RGD (cRGDFK) to PEO-*b*-P(L-lysine) to construct  $\alpha\text{v}\beta\text{3}$ -targeted micelles for effective gene delivery [30,31]. Targeted nano-carriers based on PEO-PEI have also been proposed for siRNA delivery [27,32]. Our previous study

demonstrated that PEO-*b*-P(CL-*g*-polyamine) micelles were capable of complexing siRNA and endosomal escape after cell endocytosis, leading to dose-dependent P-gp silencing effect on MDA435/LCC6 resistant cells [20]. Inspired by the structure of viral vectors that contain various proteins with different functions for cell entry, we pursued construction of peptide-modified PEO-*b*-P(CL-*g*-polyamine) and assessed the cellular delivery and transfection efficiency of complexed siRNA by these virus-like PIC micelles. The virus-related peptides, RGD and TAT, were used to modify the micellar shell. It is known that RGD motif in the penton base of adenovirus binds to  $\alpha\text{v}\beta\text{3}$  integrins on the cells leading to efficient internalization of adenovirus into cells [33]. The positively charged transduction domain of HIV-1 TAT peptide is also responsible for non-specific binding of the virus to cell membrane through tight and rapid interaction with the ubiquitous glycosaminoglycans, inducing their aggregation, which is followed by activating related mechanism for cell membrane translocation [34]. The idea of using two target molecules (e.g. TAT and monoclonal antibody) to modify micelles has also been reported by Torchilin et al. for drug delivery [35]. A fusion peptide of TAT and RGD has been used to improve DNA transfer [36].

The structures of synthesized polymers are shown in Fig. 1A. Acetal-PEO-*b*-P(CL-*g*-SP) and acetal-PEO-*b*-P(CL-*g*-DP) were synthesized from NHS-activated acetal-PEO-*b*-PCL and the compositions were confirmed by  $^1\text{H}$  NMR. The characteristic peaks corresponding to polyamine group (SP or DP) ( $\delta$  2.1–3.2 ppm), acetal ( $\delta$  1.20, 4.65), PEO ( $\delta$  3.65), and PCL ( $\delta$  1.25–2.00, 4.05) were observed indicating the successful conjugation of polyamine groups to the acetal-PEO-*b*-PCL. Based on the intensity ratio of proton peak for the polyamine groups ( $-\text{NHCH}_2-$ ) to that for the PCL segment ( $\text{OC}-(\text{CH}_2)_4-\text{CH}_2\text{O}-$ ), the polyamine substitution levels of the copolymer were estimated at 53.4 and 59.5% for acetal-PEO-*b*-P(CL-*g*-SP) and acetal-PEO-*b*-P(CL-*g*-DP), respectively. The molecular weight ( $M_n$ ) of acetal-PEO-*b*-P(CL-*g*-SP) and acetal-PEO-*b*-P(CL-*g*-DP) from  $^1\text{H}$  NMR was estimated to be 6900 and 7600, respectively.

RGD4C and TAT peptide were conjugated to the PEO terminus of acetal-PEO-*b*-P(CL-*g*-DP) by Schiff base reaction after micelle assembly. Based on the HPLC assay, less than 5% of free peptide was recovered as compared to the starting amount that was added to the micellar solution, which suggests a conjugation efficiency of 95%. The conjugation density (peptide to acetal-PEO-*b*-P(CL-*g*-DP) molar ratio) of RGD4C and TAT at the PEO terminus was calculated to be ~20%. Formation of acetal-PEO-*b*-P(CL-*g*-SP)/siRNA complexes was confirmed by agarose gel retardation assay. Consistent with our previous study [20], acetal-PEO-*b*-P(CL-*g*-SP) at 8:1 polymer:siRNA weight ratio completely complexed siRNA, and the siRNA/polymer complexes self-assembled into micelles with an average particle size of ~60 nm as indicated by DLS analysis (data not shown).

Modification of the micelle surface with peptide was achieved by incubating RGD4C- and/or TAT-decorated PEO-*b*-P(CL-*g*-DP) with acetal-PEO-*b*-P(CL-*g*-SP)/siRNA complexes (Fig. 1B). As a consequence, peptide-PEO-*b*-P(CL-*g*-DP) was inserted into the micelles by chain exchange, leading to peptide-functionalized micelles with complexed siRNA. The final ratio of polymer to siRNA for peptide-attached micelles containing siRNA was set at 16:1 (weight ratio). Peptide-attached micelles showed a unimodal distribution and larger hydrodynamic diameter (84.5–90 nm) than acetal-PEO-*b*-P(CL-*g*-SP) micelles (60 nm) (Table 1). The peptide decorated PIC micelles showed a unimodal size distribution and a hydrodynamic diameter ranging between 84.5 and 90 nm, which is comparable to viral size. The micelle formation was also confirmed by AFM using RGD-micelles as a representative structure, which showed a dehydrated diameter of 20–60 nm (Fig. 1C). The formation of mixed micelles through incubation of different micellar populations has been documented and used to modify

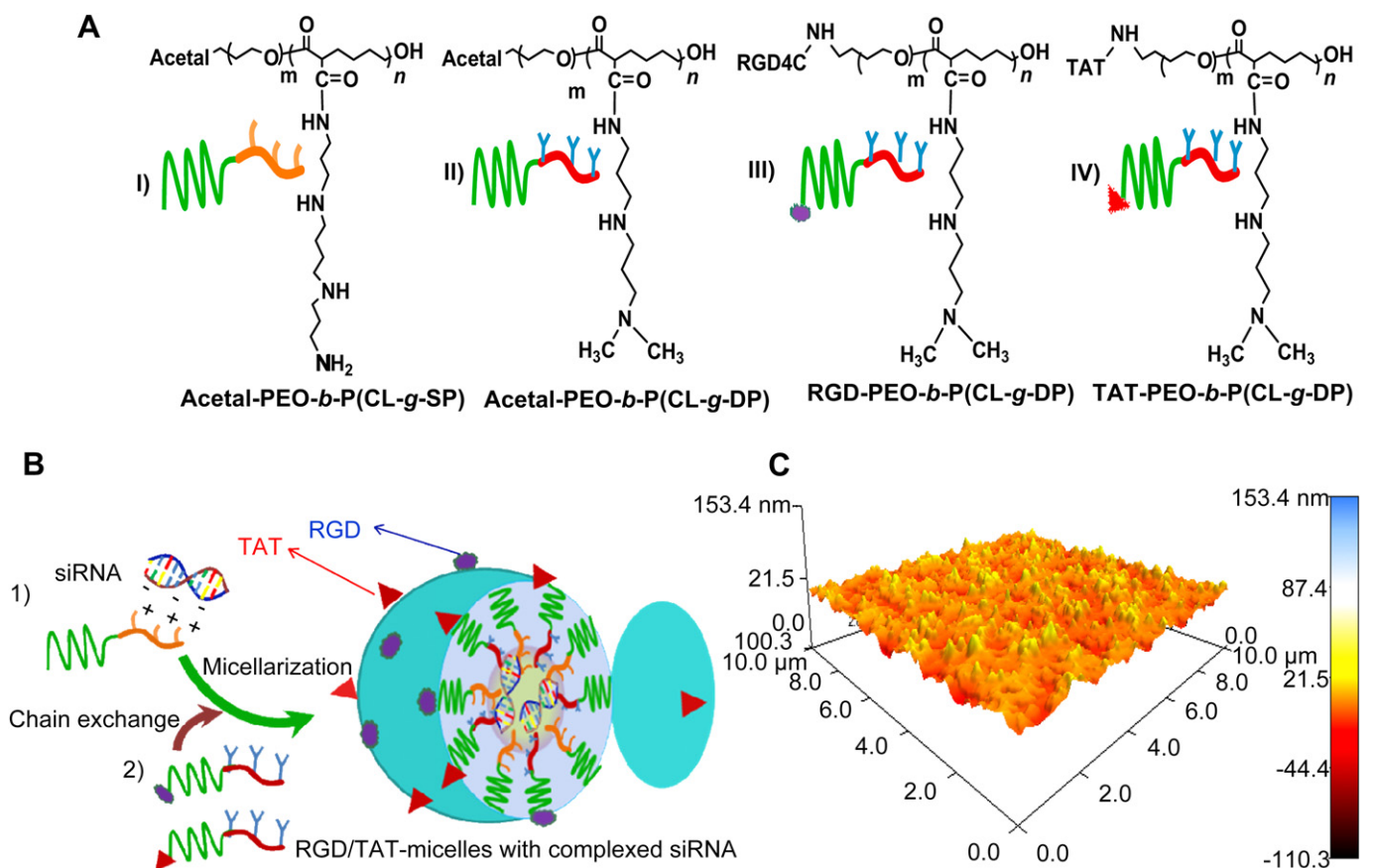


**Fig. 1.** A) Schematic structures of acetal-PEO-*b*-P(CL-g-SP) and acetal-, RGD4C- and TAT-PEO-*b*-P(CL-g-DP), B) Schematic illustration of RGD4C and/or TAT polymeric micellar siRNA complex formation: 1) acetal-PEO-*b*-P(CL-g-SP) and siRNA forms complex. 2) Incubation of the resulted siRNA complex with polymer II, III, IV or III and IV led to the preparation of NON-, RGD4C-, TAT-, and RGD4C/TAT-modified polymeric micellar siRNA complexes, respectively (compositions summarized in Table 1), C) Representative AFM image of RGD-micelles with complexed siRNA.

micellar structures in previous studies [37–39]. During incubation of two micellar populations, the exchange of single chains within the micellar structure, the unimer pool and other micellar structures present in the medium, the breakdown of large micelles into small ones (fission), and the formation of large micelles from small ones (fusion) may all occur simultaneously [40,41]. The existence of these dynamic processes leads to the formation of homogeneous mixed micelles upon mixing of different micellar populations [42]. The unimodal distribution and increased size of resulted micelles as compared to acetal-PEO-*b*-P(CL-g-SP)/siRNA micelles indicated that mixed micelles rather than two separated micellar populations were formed after incubation in this study.

FAM-siRNA was used to study the cellular uptake of micelles by MDA435/LCC6 resistant cells. As expected, both RGD4C- and TAT-functionalized micelles increased the cellular uptake of complexed siRNA by metastatic MDA435/LCC6 resistant cells, which express integrin  $\alpha v \beta 3$  on their cell membrane. Compared to NON-micelle/siRNA complexes, RGD-, TAT-, and RGD/TAT-micelles resulted in 18%, 13%, and 35% increase in the percentage of siRNA-positive cells (Fig. 2A) and produced 78%, 73% and 148% increase of mean fluorescence intensity per cell (Fig. 2B), respectively. Pre-incubation of excess free c(RGDfK) with MDA435/LCC6 resistant cells followed by the addition of RGD/TAT-micelle/FAM-siRNA was able to decrease both siRNA-positive cells and mean fluorescence intensity per cell to the level of TAT-micelle/FAM-siRNA treatment (Fig. 2A and B), pointing to the involvement of receptor mediated endocytosis in the uptake process. The cellular internalization of siRNA by micellar formulations was confirmed by confocal microscopy (Fig. 2C). The

peptide decorated micelles especially those with dual modifications appeared to be internalized better than NON-micelles by MDA435/LCC6 resistant cells.

The intracellular distribution of FAM-siRNA [22] delivered by different micellar formulations were also compared by confocal microscopy using simultaneous staining of nucleus with DAPI (blue), and endosomes/lysosomes with LysoTracker<sup>®</sup> (red) (Fig. 2D). FAM-siRNA formulated in NON- and peptide-modified micelles were observed as discrete dots partially colocalizing with the endosome/lysosomes markers as indicated by the yellow fluorescence after 4 h incubation. In addition, green fluorescence was also observed in the cytoplasmic region which was not co-localized with LysoTracker<sup>®</sup> (red), demonstrating effective endosomal escape of FAM-siRNA micelles. FAM-siRNA/Trifectin<sup>®</sup> complexes showed efficient cellular uptake and endosomal escape as well (not shown). The “proton sponge effect” provided by cationic polymers with high buffering capacity has been used to design effective siRNA vectors, although the principle is still controversial. We already showed that PEO-*b*-PCL with polyamine groups in the PCL block can cause endosome membrane disruption leading to siRNA release from the endosomes [20]. The pH-dependent endosome membrane disruption of polyamine was also reported by others [42]. In the present construct, however, more efficient endosomal escape may also be induced by the presence of TAT and RGD4C peptide [32,43–45].

We next sought to complex mdr1 siRNA into the micelle to silence P-gp expression by MDA435/LCC6 resistant cells. The relative percentage of mdr1 mRNA expression, measured by RT-PCR, for each siRNA after 48 h incubation complex compared to untreated cells

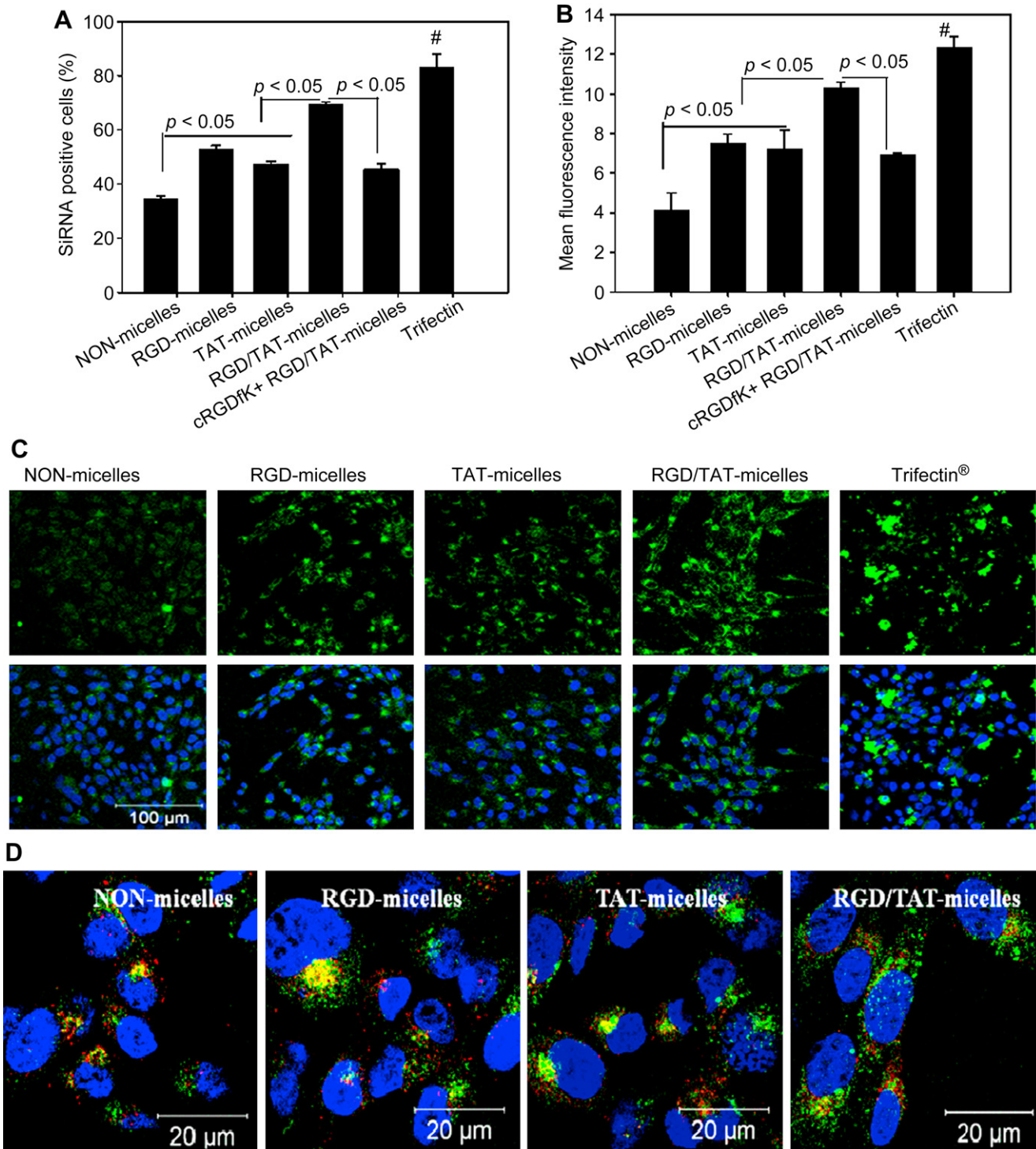


**Fig. 2.** Uptake and intracellular distribution of FAM-siRNA formulated in various polymeric micelles or Trifectin® by MDA435/LCC6 resistant cells. (A) Percentage of FAM-siRNA positive cells treated with various siRNA formulations, (B) Mean fluorescence intensity after treatment with various FAM-siRNA formulations. \* $p < 0.01$ , compared to other treatments, (C) Confocal microscopic images of MDA435/LCC6 resistant cells transfected with FAM-siRNA formulated in various micelles or in Trifectin®, (D) Intracellular distribution of the FAM-siRNA formulated in various micelles. FAM-siRNA [22] was complexed in NON-, RGD-, TAT-, and RGD/TAT-micelles, and incubated with MDA435/LCC6 resistant cells for 4 h (siRNA 200 nM). The endosomes/lysosomes and nucleus were then stained with LysoTracker® (red) and DAPI (blue), respectively.

(control) is reported in Fig. 3A. In general, mdr1 siRNA complexes were effective in down regulation of mdr1 mRNA in the following order NON-micelles < RGD-micelles = TAT-micelles < RGD/TAT-micelles. RGD- and TAT-micelles, inhibited the expression of mdr1 siRNA by ~48% and 52% at 100 nM siRNA levels, respectively, as compared to NON-micelles which caused 25% of mdr1 mRNA

inhibition ( $P < 0.05$ ). Cells transfected by RGD/TAT-micelles/mdr1 siRNA (100 nM) and Trifectin®/siRNA (40 nM) were comparable in mdr1 mRNA inhibition, showing 71% and 69% of mdr1 mRNA inhibition, respectively.

P-gp silencing activity was also evaluated at the protein level by flowcytometry and fluorescence microscopy (Fig. 3B). RGD-, TAT- and

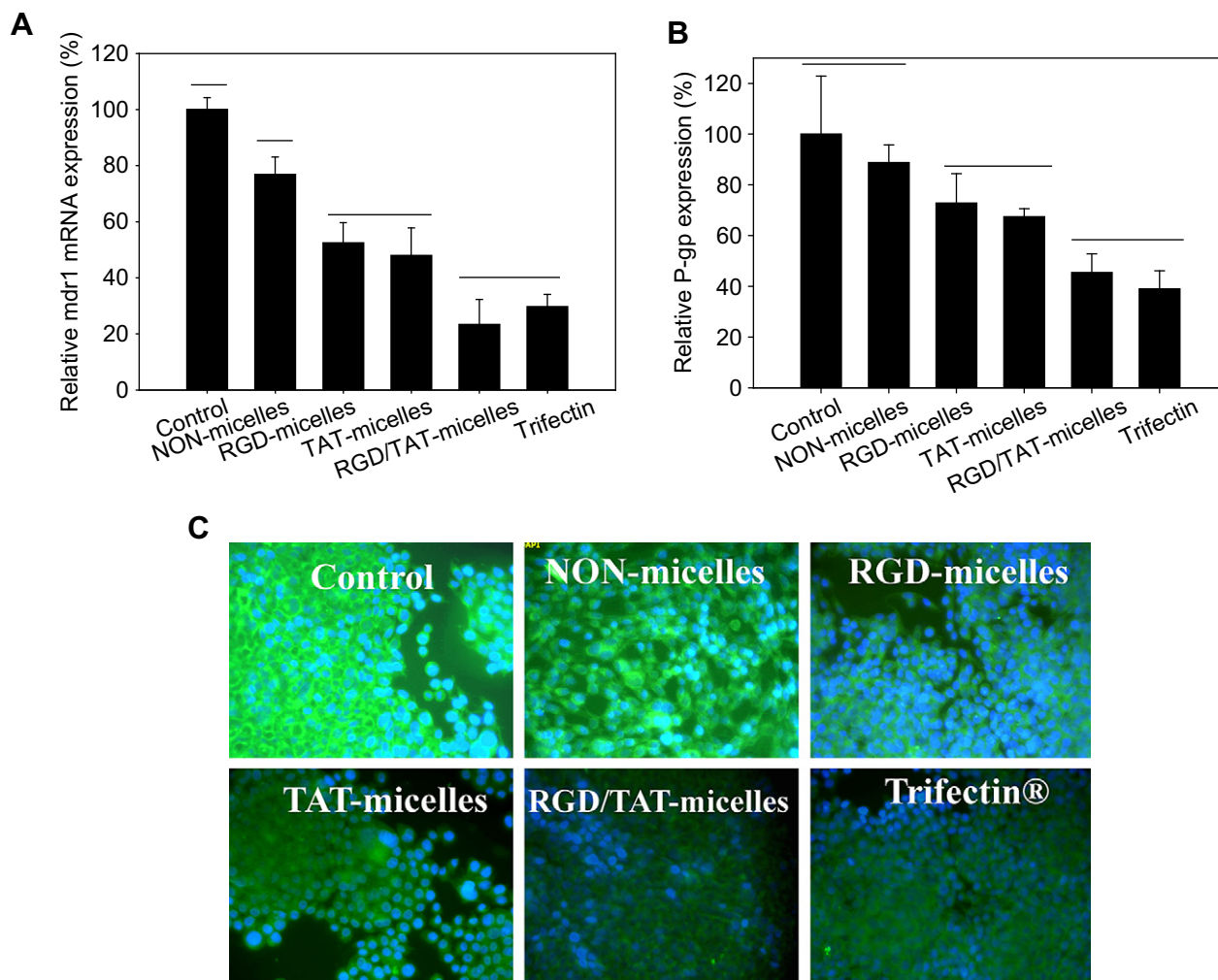


**Fig. 3.** P-gp silencing activity of the mdr1 siRNA in MDA435/LCC6 resistant cells after transfection with mdr1 siRNA formulated in various micelles or in Trifectin®. A) Real-time PCR analysis of mdr1 mRNA levels after transfection of MDA435/LCC6 cells with various polymeric micellar/siRNAs (100 nM siRNA) or Trifectin®/siRNA (40 nM siRNA) for 48 h (normalization to HPRT). Values are relative to untreated controls, B) P-gp expression by flowcytometry by comparing the P-gp related fluorescence intensity to untreated controls after 48 h incubation. Continuous lines over the data bars indicate lack of significance between groups encompassed by the lines; groups not encompassed within lines are significantly different from those encompassed by the lines (one way ANOVA followed by a post-hoc Dunnett T3 test,  $p < 0.05$ ). Each bar represents the mean  $\pm$  SD for the group. C) Fluorescence microscopy observation of P-gp silencing effect in MDA435/LCC6 resistant cells treated with micelle/siRNA using P-gp expression after staining by anti-P-gp monoclonal antibody.

RGD/TAT-micelles with complexed mdr1 siRNA showed significant P-gp silencing effect compared to control. However, P-gp down regulation by mdr1 siRNA (100 nM) complexed in NON-micelles was not significantly different from that of control at protein level ( $P > 0.05$ ). This is consistent with our previous observation [20]. Overall, the following order in the down regulation of P-gp was observed for the formulations under study: Control = NON-micelles < RGD-micelles = TAT-micelles < RGD/TAT-micelles = Trifectin®. The P-gp silencing effect was confirmed by fluorescence microscopy by comparing P-gp related fluorescence intensity after staining the cells by anti-P-gp monoclonal antibody (Fig. 3C). Consistent with flowcytometry analysis, cells transfected with NON-micelle/siRNA complexes showed slight reduction in P-gp related fluorescence compared to control, while RGD- and TAT-micelles led to significant P-gp suppression. Cells transfected with RGD/TAT-micelles at a 100 nM siRNA level showed the most effective P-gp down regulation comparable to what achieved with Trifectin® at a 40 nM siRNA level. It is not surprising that the reduction in the level of P-gp expression is less than that observed for mdr1 mRNA, given that the half-life of mRNA is much shorter than that of the corresponding protein and the siRNA silencing effect is transient. Consistent with the cell

uptake data, the RGD/TAT-micellar mdr1 siRNA complexes were more effective than either TAT- or RGD-micelles in down regulation of mdr1 mRNA and P-gp.

In further studies, the effect of P-gp down regulation by siRNA delivery systems on the intracellular accumulation and cytotoxicity of an anticancer P-gp substrate, DOX, against resistant MDA435/LCC6 cells was evaluated. Intracellular DOX accumulation in MDA435/LCC6 resistant cells transfected with mdr1 siRNA complexed with micelles or Trifectin® for 48 h was assessed by confocal microscopy (Fig. 4A). As expected, cells without mdr1 siRNA transfection as the negative control showed weak DOX fluorescence intensity in cytoplasm and cells transfected by mdr1 siRNA with Trifectin® as the positive control demonstrated strong intracellular DOX fluorescence. Compared to negative control, NON-micelles mediated transfection didn't cause DOX accumulation, while RGD-, TAT- and RGD/TAT-micelles mediated transfection of mdr1 siRNA significantly increased intracellular DOX fluorescence (Fig. 4A). It is worth noting that DOX fluorescence was also observed in the nuclei of cells after transfection of mdr1 siRNA with peptide-modified micelles, in particular RGD/TAT-micelles which showed similar effects on DOX cellular accumulation to that of

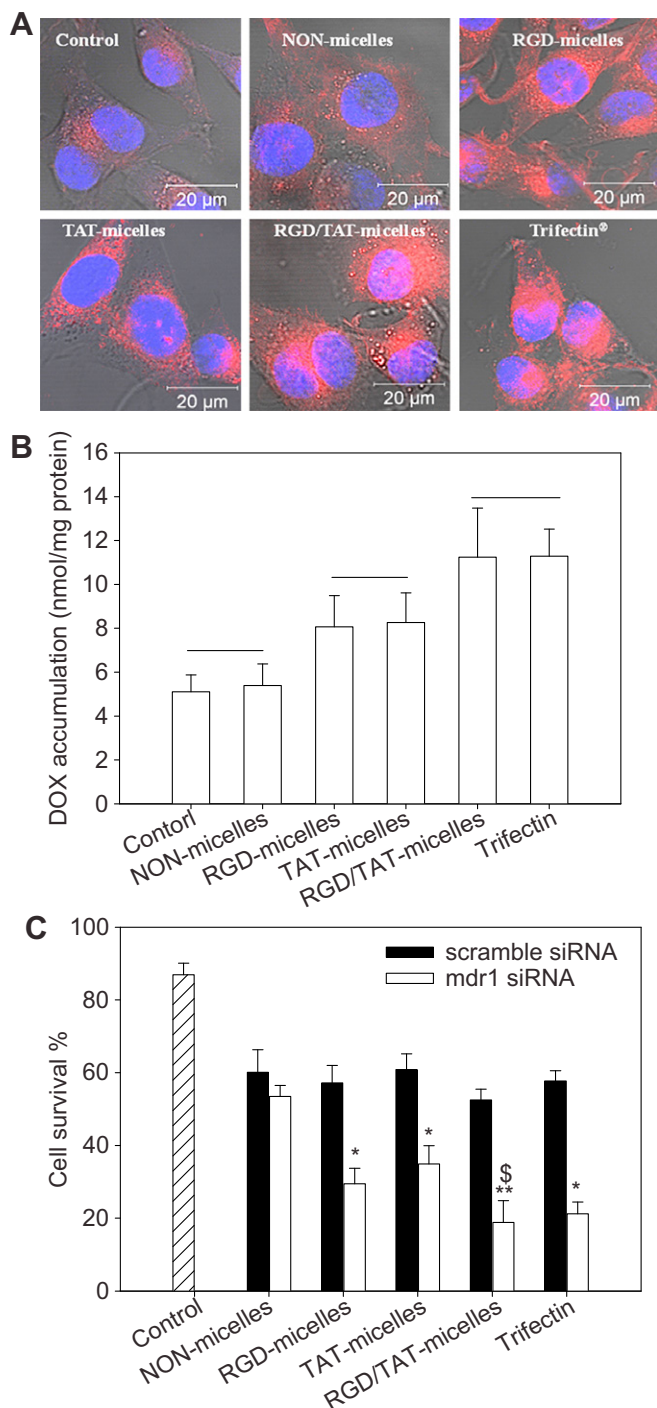


**Fig. 4.** Reversal of resistance to DOX in MDA435/LCC6 resistant cells after transfection with *mdr1* siRNA formulations. Cells without transfection were used as the control. After transfection, the cells were exposed to free DOX ( $5 \mu\text{g mL}^{-1}$ ) and assessed for (A) DOX cellular accumulation and distribution by fluorescence microscopy. After 4 h of incubation with free DOX, the cells were washed, fixed, and stained with DAPI for confocal microscopy observation, (B) DOX cellular accumulation by fluorescence spectroscopy. After 4 h of incubation with free DOX, the cells were washed, lysed and DOX accumulation was quantified by a microplate fluorometer. Continuous lines over the data bars indicate lack of significance between groups encompassed by the lines; groups not encompassed within lines are significantly different from those encompassed by the lines (one way ANOVA followed by a post-hoc Dunnett T3 test,  $p < 0.05$ ). Each bar represents the mean  $\pm$  SD for the group, (C) Cell viability by MTT assay. After 48 h of incubation with free DOX ( $5 \mu\text{g mL}^{-1}$ ), cytotoxicity of DOX against MDA435/LCC6 resistant cells was evaluated by MTT assay. \* $P < 0.05$ , \*\* $P < 0.01$ , compared to NON-micelles;  $^{\$}P < 0.05$ , compared to RGD- and TAT-micelles.

Trifectin®. Since it has been shown that the nuclear membrane also expresses P-gp [46], DOX penetration in the nuclei of cells treated with siRNA complexes may indicate effective down regulation of P-gp on nuclei membrane. Intracellular DOX accumulation was then quantified by fluorescence spectroscopy (Fig. 4B). The quantitative results from fluorometer were in good agreement with the qualitative results obtained from fluorescent microscopy. Compared to untreated cells or NON-micelle transfected cells, RGD- and TAT-micelles transfection led to  $\sim 60\%$  increase in DOX accumulation, while RGD/TAT-micelles and Trifectin® mediated transfection resulted in  $\sim 100\%$  increase in DOX accumulation.

In light of these results we then assessed the effects of *mdr1* silencing on the cytotoxicity of DOX after 48 h incubation with cells. As shown in Fig. 4C, transfection of *mdr1* siRNA with peptide-modified micelles or Trifectin® significantly enhanced DOX cytotoxicity against MDA435/LCC6 resistant cells. In the presence of DOX ( $5 \mu\text{g mL}^{-1}$ ), viability of cells with *mdr1* siRNA transfection using various carriers ranked as control (no siRNA) (90%) > NON-micelles (53.4%) > RGD-micelles (29.5%) = TAT-micelles (34.9%) > RGD/TAT-micelles (18.9%) = Trifectin® (21.4%). The carriers showed non-specific toxicity against MDA435/LCC6 resistant cells. The percentage of viable cells after transfection with scrambled siRNA complexed with all carriers was around 60%. It should be noted that even the highest silencing effect achieved by RGD/TAT-micelles, resistance to DOX was not completely reversed. At the same DOX concentration, 100% inhibition in growth of sensitive MDA435/LCC6 cells was observed compared to 80% inhibition in cell growth achieved by DOX when resistant cells were pretreated with RGD/TAT-micellar *mdr1* siRNA complexes (data not shown). Furthermore, in sensitive cells, DOX was mainly distributed in the nuclei, in contrast to what observed in resistant cells. The observation points to the importance of silencing P-gp expression on the membrane of cell organelles for the reversal of DOX resistance.

Despite the marked P-gp silencing activity achieved particularly by RGD/TAT-micellar complexes in vitro, a successful in vivo silencing effect is greatly dependent on an effective accumulation of siRNA in the cancer cells after systemic administration. The RGD-mediated specific recognition of RGD/TAT-micelles, followed by TAT-facilitated non-specific cellular penetration is likely to provide efficient gene silencing effect in metastatic cancer cells that express  $\alpha_v\beta_3$  integrins, in vivo, only if the micellar siRNA carrier can reach the tumor cells in sufficient level. This will very well be dependent on the stability of the siRNA micellar complex and its pharmacokinetic profile. Our future work will explore the use of this micellar siRNA delivery in vivo paying special attention to the bio-distribution of peptide-functionalized micellar siRNA complexes after systemic administration.

#### 4. Conclusions

We have described the design, synthesis and evaluation of the PEO-*b*-polyester based virus-like micelles containing a biodegradable polycationic core and a peptide-functionalized shell for targeted siRNA delivery with high transfection efficiency. We demonstrated that RGD- and/or TAT-modification increased cellular uptake of siRNA formulated micelles. These peptide-functionalized micelles, especially RGD/TAT-micelles containing *mdr1* siRNA effectively silenced P-gp expression, increased DOX intracellular uptake, improved DOX penetration into nuclei and finally enhanced DOX cytotoxicity in MDA435/LCC6 DOX resistant cells. The results of this study demonstrated a promise for peptide modified PEO-*b*-P(CL-polyamine) micelles as non-viral vehicle for efficient siRNA delivery to its cellular and molecular targets.

## Acknowledgement

This research was funded by research grants from Natural Science and Engineering Research Council of Canada (NSERC) and Canadian Institute of Health Research (CIHR). We thank Dr. Jianfei Wang and Ms. Yue Huang (Division of Plastic and Reconstructive Surgery, University of Alberta) for their technical help in real time-PCR.

## Appendix

Figures with essential color discrimination. Figs. 1–4 in this article are difficult to interpret in black and white. The full color images can be found in the on-line version at doi:10.1016/j.biomaterials.2010.03.075.

## References

- [1] Hammond SM, Caudy AA, Hannon GJ. Post-transcriptional gene silencing by double-stranded RNA. *Nat Rev Genet* 2001;2:110–9.
- [2] de Fougerolles A, Vornlocher HP, Maraganore J, Lieberman J. Interfering with disease: a progress report on siRNA-based therapeutics. *Nat Rev Drug Discov* 2007;6:443–53.
- [3] Honma K, Iwao-Koizumi K, Takeshita F, Yamamoto Y, Yoshida T, Nishio K, et al. RPN2 gene confers docetaxel resistance in breast cancer. *Nat Med* 2008;14:939–48.
- [4] Pirolo KF, Chang EH. Targeted delivery of small interfering RNA: approaching effective cancer therapies. *Cancer Res* 2008;68:1247–50.
- [5] Aagaard L, Rossi JJ. RNAi therapeutics: principles, prospects and challenges. *Adv Drug Deliv Rev* 2007;59:75–86.
- [6] Whitehead KA, Langer R, Anderson DG. Knocking down barriers: advances in siRNA delivery. *Nat Rev Drug Discov* 2009;8:129–38.
- [7] Juliano R, Alam MR, Dixit V, Kang H. Mechanisms and strategies for effective delivery of antisense and siRNA oligonucleotides. *Nucleic Acids Res* 2008;36:4158–71.
- [8] Kawakami S, Hashida M. Targeted delivery systems of small interfering RNA by systemic administration. *Drug Metab Pharmacokinet* 2007;22:142–51.
- [9] Sanguino A, Lopez-Berestein G, Sood AK. Strategies for in vivo siRNA delivery in cancer. *Mini Rev Med Chem* 2008;8:248–55.
- [10] Soutschek J, Akinc A, Bramlage B, Charisse K, Constien R, Donoghue M, et al. Therapeutic silencing of an endogenous gene by systemic administration of modified siRNAs. *Nature* 2004;432:173–8.
- [11] Bartlett DW, Su H, Hildebrandt IJ, Weber WA, Davis ME. Impact of tumor-specific targeting on the biodistribution and efficacy of siRNA nanoparticles measured by multimodality in vivo imaging. *Proc Natl Acad Sci U S A* 2007;104:15549–54.
- [12] Gary DJ, Puri N, Won YY. Polymer-based siRNA delivery: perspectives on the fundamental and phenomenological distinctions from polymer-based DNA delivery. *J Control Release* 2007;121:64–73.
- [13] Kumar LD, Clarke AR. Gene manipulation through the use of small interfering RNA (siRNA): from in vitro to in vivo applications. *Adv Drug Deliv Rev* 2007;59:87–100.
- [14] Schaffer DV, Fidelman NA, Dan N, Lauffenburger DA. Vector unpacking as a potential barrier for receptor-mediated polyplex gene delivery. *Biotechnol Bioeng* 2000;67:598–606.
- [15] Edelstein ML, Abedi MR, Wixon J. Gene therapy clinical trials worldwide to 2007—an update. *J Gene Med* 2007;9:833–42.
- [16] Smaglik P. Merck blocks 'safer' gene therapy trials. *Nature* 2000;403:817.
- [17] Aliabadi HM, Brocks DR, Lavasanifar A. Polymeric micelles for the solubilization and delivery of cyclosporine A: pharmacokinetics and biodistribution. *Biomaterials* 2005;26:7251–9.
- [18] de Fougerolles AR. Delivery vehicles for small interfering RNA in vivo. *Hum Gene Ther* 2008;19:125–32.
- [19] Jeong JH, Kim SW, Park TG. Molecular design of functional polymers for gene therapy. *Prog Polym Sci* 2007;32:1239–74.
- [20] Xiong XB, Uludag H, Lavasanifar A. Biodegradable amphiphilic poly(ethylene oxide)-block-polyesters with grafted polyamines as supramolecular nano-carriers for efficient siRNA delivery. *Biomaterials* 2009;30:242–53.
- [21] Svoboda P. Off-targeting and other non-specific effects of RNAi experiments in mammalian cells. *Curr Opin Mol Ther* 2007;9:248–57.
- [22] Leonessa F, Green D, Licht T, Wright A, Wingate-Legette K, Lippman J, et al. MDA435/LCC6 and MDA435/LCC6MDR1: ascites models of human breast cancer. *Br J Cancer* 1996;73:154–61.
- [23] Wong HL, Bendayan R, Rauth AM, Xue HY, Babakhanian K, Wu XY. A mechanistic study of enhanced doxorubicin uptake and retention in multidrug resistant breast cancer cells using a polymer–lipid hybrid nanoparticle system. *J Pharmacol Exp Ther* 2006;317:1372–81.
- [24] Xiong XB, Mahmud A, Uludag H, Lavasanifar A. Multifunctional polymeric micelles for enhanced intracellular delivery of doxorubicin to metastatic cancer cells. *Pharm Res* 2008;25:2555–66.
- [25] Xiong XB, Mahmud A, Uludag H, Lavasanifar A. Conjugation of arginine-glycine-aspartic acid peptides to poly(ethylene oxide)-*b*-poly(epsilon-caprolactone) micelles for enhanced intracellular drug delivery to metastatic tumor cells. *Biomacromolecules* 2007;8:874–84.
- [26] Itaka K, Kanayama N, Nishiyama N, Jang WD, Yamasaki Y, Nakamura K, et al. Supramolecular nanocarrier of siRNA from PEG-based block cationic carrying diamine side chain with distinctive pK(a) directed to enhance intracellular gene silencing. *J Am Chem Soc* 2004;126:13612–3.
- [27] Kim SH, Jeong JH, Cho KC, Kim SW, Park TG. Target-specific gene silencing by siRNA plasmid DNA complexed with folate-modified poly(ethylenimine). *J Control Release* 2005;104:223–32.
- [28] Lee SH, Kim SH, Park TG. Anticancer effect by intratumoral and intravenous administration of VEGF siRNA polyelectrolyte complex micelles. *J Biotechnol* 2007;131:S48–9.
- [29] Nishiyama N, Kataoka K. Current state, achievements, and future prospects of polymeric micelles as nanocarriers for drug and gene delivery. *Pharmacol Ther* 2006;112:630–48.
- [30] Oba M, Aoyagi K, Miyata K, Matsumoto Y, Itaka K, Nishiyama N, et al. Polyplex micelles with cyclic RGD peptide ligands and disulfide cross-links directing to the enhanced transfection via controlled intracellular trafficking. *Mol Pharmacol* 2008;5:1080–92.
- [31] Oba M, Fukushima S, Kanayama N, Aoyagi K, Nishiyama N, Koyama H, et al. Cyclic RGD peptide-conjugated polyplex micelles as a targetable gene delivery system directed to cells possessing alphavbeta3 and alphavbeta5 integrins. *Bioconjug Chem* 2007;18:1415–23.
- [32] Suk JS, Suh J, Choy K, Lai SK, Fu J, Hanes J. Gene delivery to differentiated neurotypic cells with RGD and HIV Tat peptide functionalized polymeric nanoparticles. *Biomaterials* 2006;27:5143–50.
- [33] Medina-Kauwe LK. Endocytosis of adenovirus and adenovirus capsid proteins. *Adv Drug Deliv Rev* 2003;55:1485–96.
- [34] Bayer P, Kraft M, Ejchart A, Westendorp M, Frank R, Rosch P. Structural studies of HIV-1 Tat protein. *J Mol Biol* 1995;247:529–35.
- [35] Sawant RM, Hurley JP, Salmaso S, Kale A, Tolcheva E, Levchenko TS, et al. "SMART" drug delivery systems: double-targeted pH-responsive pharmaceutical nanocarriers. *Bioconjug Chem* 2006;17:943–9.
- [36] Renigunta A, Krasteva G, Konig P, Rose F, Klepetko W, Grimminger F, et al. DNA transfer into human lung cells is improved with Tat-RGD peptide by caveoli-mediated endocytosis. *Bioconjug Chem* 2006;17:327–34.
- [37] Gao Z, Fain HD, Rapoport N. Ultrasound-enhanced tumor targeting of polymeric micellar drug carriers. *Mol Pharmacol* 2004;1:317–30.
- [38] Liu TB, Nace VM, Chu B. Self-assembly of mixed amphiphilic triblock copolymers in aqueous solution. *Langmuir* 1999;15:3109–17.
- [39] Vakil R, Kwon GS. Poly(ethylene glycol)-*b*-poly(epsilon-caprolactone) and PEG-phospholipid form stable mixed micelles in aqueous media. *Langmuir* 2006;22:9723–9.
- [40] Smith CK, Liu GJ. Determination of the rate constant for chain insertion into poly(methyl methacrylate)-block-poly(methacrylic acid) micelles by a fluorescence method. *Macromolecules* 1996 Mar 11;29(6):2060–7.
- [41] Vangeyete P, Leyh B, Heinrich M, Grandjean J, Bourgaux C, Jerome R. Self-assembly of poly(ethylene oxide)-*b*-poly(epsilon-caprolactone) copolymers in aqueous solution. *Langmuir* 2004;20:8442–51.
- [42] Wang XL, Nguyen T, Gillespie D, Jensen R, Lu ZR. A multifunctional and reversibly polymerizable carrier for efficient siRNA delivery. *Biomaterials* 2008;29:15–22.
- [43] Ferrer-Miralles N, Vazquez E, Villaverde A. Membrane-active peptides for non-viral gene therapy: making the safest easier. *Trends Biotechnol* 2008;26:267–75.
- [44] Nativo P, Prior IA, Brust M. Uptake and intracellular fate of surface-modified gold nanoparticles. *ACS Nano* 2008;2:1639–44.
- [45] Shayakhmetov DM, Eberly AM, Li ZY, Lieber A. Deletion of penton RGD motifs affects the efficiency of both the internalization and the endosome escape of viral particles containing adenovirus serotype 5 or 35 fiber knobs. *J Virol* 2005;79:1053–61.
- [46] Maraldi NM, Zini N, Santi S, Scotlandi K, Serra M, Baldini N. P-glycoprotein subcellular localization and cell morphology in MDR1 gene-transfected human osteosarcoma cells. *Biol Cell* 1999;91:17–28.